AD-A118 279 FOREIGN TECHNOLOGY DIV WRIGHT-PATTERSON AFB OH F/G 20/4
ANALYTICAL AND EXPERIMENTAL INVESTIGATION OF PERFORMANCE OF SUP--ETC(U)
JUL 82 S HUILI, C ZHONGQING
UNCLASSIFIED FTD-ID(RS)T-0347-82 NL

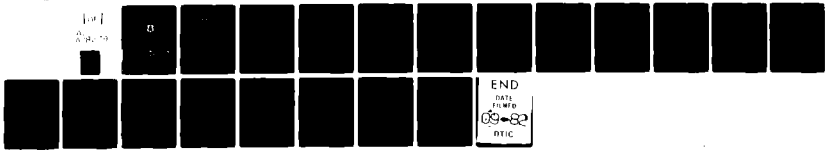

END
DATE FILMED
DTIC

FTD-ID(RS)T-0347-82

FOREIGN TECHNOLOGY DIVISION

ANALYTICAL AND EXPERIMENTAL INVESTIGATION OF PERFORMANCE OF SUPERSONIC EJECTOR NOZZLES

by

Shen Huili and Chen Zhongqing

Approved for public release;
distribution unlimited.

EDITED TRANSLATION

FTD-ID(RS)T-0347-82 21 July 1982

MICROFICHE NR: FTD-82-C-000986

ANALYTICAL AND EXPERIMENTAL INVESTIGATION OF PERFORMANCE OF SUPERSONIC EJECTOR NOZZLES

By: Shen Huili and Chen Zhongqing

English pages: 17

Source: Attachment to IR 1 572 0090 79, pp. 51-63; 1 unn pg

Country of origin: China
Translated by: SCITRAN
F33657-81-D-0263
Requester: FTD/TQTD

PREPARED BY:

TRANSLATION DIVISION
FOREIGN TECHNOLOGY DIVISION
WP-AFB, OHIO.

GRAPHICS DISCLAIMER

All figures, graphics, tables, equations, etc. merged into this translation were extracted from the best quality copy available.

ANALYTICAL AND EXPERIMENTAL INVESTIGATION OF PERFORMANCE OF SUPERSONIC EJECTOR NOZZLES

Shen Huili and Chen Zhongqing

This paper presents an analytical method for calculating the flow field and performance of supersonic ejector nozzles. The calculations involve the real sonic line at the exit of the primary nozzle, the inviscid primary flow field, the correction for the viscosity effect, the pumping characteristic and the thrust characteristic.

In order to have the calculated results agree with the experimental data, the real sonic line, instead of the plane sonic line, is taken as the initial base line of calculations. The real sonic line is obtained by joining the points of intersection of constant flow angle lines (isoclines) and the throat region with Mach lines at the lip of the primary nozzle.

The inviscid primary flow field of the nozzle is calculated at first and then a correction is made to account for the viscous effect. The method of correction for the viscous effect proposed in this paper replaces the original geometric coordinates of the ejector shroud with the corrected geometric coordinates which are obtained by superimposing on the original geometric coordinates the displacements of the mixed region and the boundary layer. On the basis of the corrected coordinates, the actual primary flow field and pumping performance of the nozzle are then calculated. The proposed method proves to be quite simple and accurate .

Calculations were performed on a 320 digital computer and model tests were conducted on a ground test facility. The analytical and experimental results are found to be in fairly satisfactory agreement.

For a relatively high secondary flow rate, the primary flow continues to accelerate and expand in the divergent section of the "fluid wall boundary" after leaving the primary nozzle, while the secondary flow accelerates in the passage formed between the shroud and the

FLOW CONFIGURATION [1] [2]

Ejector nozzle with high secondary flow rate (Figure 1)

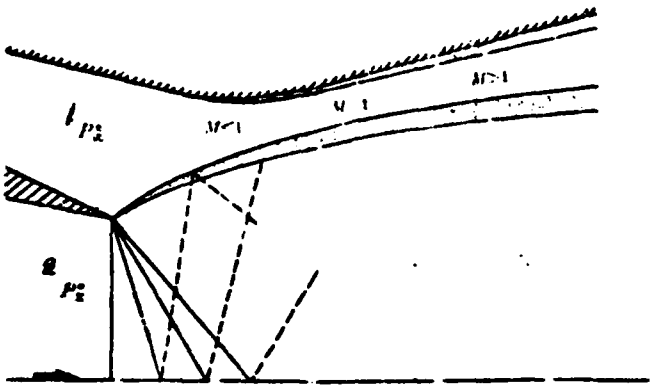

Figure 1. Flow configuration in ejector nozzle with high secondary flow rate
Key: 1--secondary; 2--primary

"fluid boundary". Depending on the dimension of the nozzle and the upstream flow conditions, there are three possibilities:
the secondary flow remains subsonic;
the secondary flow becomes sonic at the exit plane of the nozzle;
the secondary flow becomes supersonic at the exit plane of the nozzle.

Due to the viscosity of the gas, a mixing layer of variable pressure is formed between the primary flow and the secondary flow and a boundary layer is formed along the shroud. However, the viscous effect is relatively small for a high secondary flow rate.

For a very low secondary flow rate (approaching zero), the primary flow practically expands as a free jet into a region of constant pressure. The free jet boundary almost sticks to the divergent section of the shroud and is recompressed to produce a shock. Upstream of the compression region, the low speed, constant pressure flow restricted by the constant pressure jet boundary forms a dead region. Due to the viscous effect, a mixing region forms along the boundary of the primary flow. Mass and energy transfers between the

Flow configuration with secondary flow rate (Figure 2)

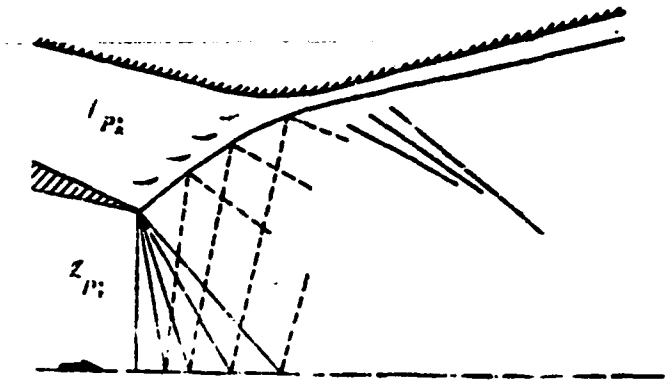

Figure 2. Flow configuration of the ejector nozzle with low secondary flow rate
Key: 1--secondary; 2--primary

primary and the secondary flows occur in this mixing region. The primary flow continuously drags out a certain flow rate from the dead region. This flow rate is provided by the supply system of the secondary flow.

METHOD OF CALCULATION

1. Calculation of the real sonic line [3]

The real sonic line must be determined after the flow angles at the transonic throat region of the primary nozzle and the Mach lines generating from the lip of the primary nozzle are calculated (Figure 3). Assuming that the flow is steady, irrotational, isentropic and two-dimensional, it can be described in terms of the stream function by:

$$\left[1-\left(\frac{v}{a}\right)^2\cdot\frac{u^2}{a^2}\right]\psi_{xx}-\left[2\left(\frac{v}{a}\right)^2\frac{uv}{a^2}\right]\psi_{xy}$$

$$+\left[1-\left(\frac{v}{a}\right)^2\frac{v^2}{a^2}\right]\psi_{yy}=0 \qquad (1)$$

where the subscripts denote the derivatives in the x and y directions. The following velocity variables are introduced:

$$q=(u^2+v^2)^{\frac{1}{2}} \qquad (2)$$

$$\theta=\arctan\left(\frac{v}{u}\right) \qquad (3)$$

Then equation (1) becomes:

$$\frac{\partial}{\partial q}\left(\frac{\rho}{\rho}+\frac{\partial \Phi}{\partial q}\right)+\frac{\rho}{\rho}\frac{1}{q}\left(1-\frac{q^2}{a^2}\right)\frac{\partial^2 \Phi}{\partial \theta^2}=0. \qquad (4)$$

Again introducing the transformed velocity defined by:

$$d\omega=\frac{\rho}{\rho_0}\frac{dq}{q} \qquad (5)$$

the above equation is simplified into

$$\frac{\partial^2 \Phi}{\partial \omega^2}+K(M)\frac{\partial^2 \Phi}{\partial \theta^2}=0, \qquad (6)$$

$$K(M)=\left(\frac{\rho_0}{\rho}\right)^2(1-M^2) \qquad (7)$$

where

Upon introducing the "tangent gas approximation", i.e., K(M) = 1, the hodograph relation (6) is simplified into the Cauchy-Riemann equation. Hence, the flow field can be solved by complex variable techniques. The incompressible and compressible flows are related by the transformation

$$d\omega=\frac{\rho}{\rho_0}\frac{dq}{q}$$

upon direct integration

$$\omega=\ln\frac{2\left(\frac{q}{q_m}\right)\sqrt{1-M_m^2}}{1+\sqrt{1+\left(\frac{q}{q_m}\right)^2 M_m^2}} \qquad (8)$$

where q_m and M_m represent the velocity and the Mach number at the matching state. Since the Cauchy-Riemann condition is satified, a set of sources and sinks satisfying the required boundary conditions is employed to determine the complex potential function:

$$F(\omega-i\theta)=\ln\frac{\cosh\frac{\pi}{a}(\omega-i\theta-\omega_1)-\cosh\left(\frac{\pi}{a}\Delta\omega\right)}{\cosh\frac{\pi}{a}(\omega-i\theta-\omega_1)-1} \qquad (9)$$

where $\Delta\omega=\omega_1-\omega_2$. Upon differentiating the above equation, the complex velocity is obtained:

$$\frac{dF}{d(\omega-i\theta)}=\frac{\frac{\pi}{a}\sinh\frac{\pi}{a}(\omega-i\theta-\omega_1)}{\cosh\frac{\pi}{a}(\omega-i\theta-\omega_1)-\cosh\left(\frac{\pi}{a}\Delta\omega\right)} \qquad (10)$$

$$-\frac{\frac{\pi}{a}\sinh\frac{\pi}{a}(\omega-i\theta-\omega_1)}{\cosh\frac{\pi}{a}(\omega-i\theta-\omega_1)-1} \qquad (10)$$

Upon applying this solution to the conical nozzle and introducing the complex variable z=x+iy, the hodograph plane can be transformed into the physical plane. Hence

$$dz = \frac{1}{e^{\omega-\bar{\omega}} \cdot d(\omega - i\theta)} \cdot \frac{dF}{d(\omega - i\theta)} \cdot d(\omega - i\theta) - \frac{e^{\omega-\bar{\omega}}}{4} \cdot \overline{\frac{dF}{d(\omega - i\theta)}} \cdot d(\omega - i\theta) \qquad (11)$$

where the bar over the last term denotes that the complex conjugate is to be taken. Integration of equation (11) gives the physical location (x,y) of any point in the hodograph plane. The constant of integration can be determined by assigning the physical location (0,1) to correspond to the nozzle lip (ω_j, a) in the hodograph plane. The distribution of the flow angle in the throat region is particularly useful. The lines of constant flow angle are also called "isoclines". In order to obtain the equation for the isoclines, equation (11) is integrated numerically from ω_a to ω_j for selected values of the flow angle between 0 and a.

The method of characteristics is employed to calculate the Mach lines generated from the nozzle lip. The characteristic equations are:

$$\frac{dy}{dx} = \tan(\theta \pm \mu) \qquad (12)$$

$$\frac{dp}{\rho q^2 \tan\mu} \pm d\theta + \frac{\sin\theta \cdot \sin\mu}{\sin(\theta \pm \mu)} \cdot \frac{dy}{y} = 0 \qquad (13)$$

$$\frac{dy}{dx} = \tan\theta \qquad (14)$$

where μ is the local Mach angle. The static pressure p and the flow angle θ are chosen as the independent variables. The expansion at the nozzle lip is of the centered wave type and satisfies the Prandtl-Meyer function. The flow at the nozzle lip turns through the Prandtl-Meyer angle, and this expansion process is divided into a finite number of discrete steps. The first point on the sonic line is the point of intersection of the first isocline and the first Mach line originating from the nozzle lip (Figure 3). The locations of the other points on the sonic line are determined in the same fashion.

2. Calculation of the inviscid flow field and the characteristics for high secondary flow rate

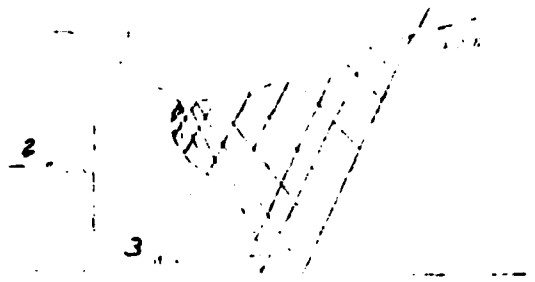

Figure 3. Real sonic line
Key: 1--jet boundary; 2--isoclines; 3--sonic line

(1) Assumptions:

The secondary flow is a one-dimensional isentropic flow; the static pressure along the "fluid boundary" between the primary flow and the secondary flow is common on both sides; the primary flow is inviscid and is subjected to the influence of the characteristics.

(2) Given conditions:

stagnation pressure, stagnation temperature and mass flow rate of the primary flow;
stagnation pressure and stagnation temperature of the secondary flow;
ambient pressure;
geometric dimensions of the ejector nozzle.

(3) Principal equations applied [5]:

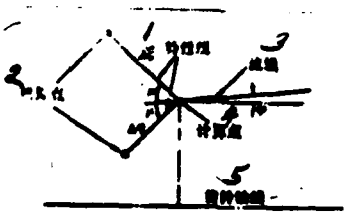

Figure 4. Calculation scheme for the ejector nozzle
Key: 1--characteristics; 2--determined points; 3--streamline; 4--calculation point; 5--axis of revolution

$$G = mA\sigma(\lambda)\frac{P^*}{\sqrt{T^*}} \qquad (15)$$

$$\theta = \text{Arc sin}\frac{1}{M} \qquad (16)$$

$$\lambda^2 = 1 + K\frac{2}{K-1}\sin^2\left(\sqrt{\frac{K-1}{K+1}}\theta\right) \qquad (17)$$

$$\frac{\delta p}{p}\frac{\sqrt{M^2-1}}{KM^2} + \delta\phi = -\frac{\sin\phi}{MR}\delta n \qquad (18)$$

$$\frac{\delta p}{p}\frac{\sqrt{M^2-1}}{KM^2} - \delta\phi = -\frac{\sin\phi}{MR}\delta L \qquad (19)$$

(4) Calculation procedures: An arbitrary secondary mass flow rate is taken. Based on the condition of equal static pressure for the primary flow and the secondary flow at the exit of the primary nozzle, the expansion fan is determined. The location of the "fluid boundary" is determined by iteration. The continuity equation is written for each section along the secondary flow, while the equation for the characteristic originating from this point is written at the same time. The calculation is conducted until the nozzle exit is reached. If the static pressure of the secondary flow at the nozzle exit is found to be the same as the ambient pressure, the secondary flow is subsonic. If in case the secondary flow is found to be supersonic at the exit, then there exists a throat section in the secondary flow where the Mach number is 1. The mass flow rate selected must then be modified such that it is equal to the choked flow rate.

3. Correction for viscous effect [4], [3], [7]

Reference [4] included the viscous effect by correcting the cross sectional area of the throat of the secondary flow. [3], on the other hand, corrected the boundary between the two flows and included the boundary layer along the shroud. The former is simpler but less accurate, and the latter method is more complicated. The present paper proposes the shroud coordinates correction method, which can be described as:

(1) calculation of the inviscid flow field with the initial dimension of the shroud of the ejector;

(2) calculation of the displacement thickness of the mixing region between the primary flow and the secondary flow;

(3) calculation of the boundary layer displacement thickness along the inner wall of the shroud;
(4) correction of the throat section of the secondary flow by subtracting the boundary layer displacement thickness from the original throat section dimension and adding to it the mixing layer displacement thickness;
(5) based on the corrected shroud coordinates, the entire flow field is calculated again by the inviscid method. The analysis is described in detail below.

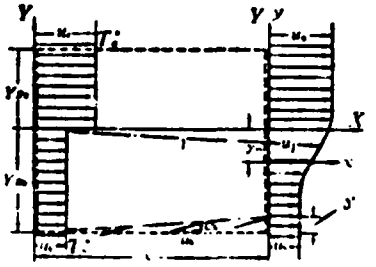

Figure 5. Velocity profile in the mixing region

(1) Calculation of the displacement thickness δ_1^* of the secondary flow in the mixing layer

If the mixing layer is assumed to be a constant-pressure region, the velocity profile in the mixing layer (Figure 5) can be obtained by the following equation [4]:

$$\frac{u}{u_a} = \frac{1+\varphi_0}{2} + \frac{1-\varphi_0}{2}\left(\frac{1}{\sqrt{\pi}}\int_0^{\eta} e^{-\beta^2}\cdot d\beta\right) = \frac{1+\varphi_0}{2} + \frac{1-\varphi_0}{2}\,\mathrm{erf}\,\eta \qquad (30)$$

where $\varphi_0 = \frac{u_b}{u_a}$,

u_b - velocity of the secondary flow
u_a - velocity of the primary flow;
u - velocity component in the x direction

$\mathrm{erf}\,\eta = \frac{2}{\sqrt{\pi}}\int_0^{\eta} e^{-\beta^2}\cdot d\beta$,

$\eta = \sigma\frac{y}{x}$, σ - similarity parameter, given by a semi-empirical formula; y,x - physical coordinates in the mixing layer; velocity at the point y = 0: $u = \frac{u_a + u_b}{2}$ (that is $\eta = 0$, $\mathrm{erf}\,\eta = 0$, $\frac{u}{u_a} = \frac{1+\varphi_0}{2}$).

η is the similarity coordinate, that is, for equal values of $\frac{y}{x}$; then the $\frac{u}{u_a}$ value is also the same. In other words, the velocity profile at each section of the mixing layer is similar.

Upon taking the Prandtl number as 1, neglecting $\frac{\partial p}{\partial x}$, and assuming C_p to be constant, the temperature profile can be obtained from the velocity profile directly, that is

$$\frac{T^*}{T_a^*} = \frac{1}{1-\varphi_1}\left[\left(\frac{T_b^*}{T_a^*}-\varphi_1\right)+\left(1-\frac{T_b^*}{T_a^*}\right)\varphi\right] \qquad (21)$$

where T^* - stagnation temperature of the mixing region; T_a^* - stagnation temprature of the primary flow; T_b^* - stagnation temperature of the secondary flow.

Given the velocity, stagnation temperature and static pressure (equal to the static pressure of the primary and secondary flows at the boundary of the mixing layer) at each point of the mixing layer, the displacement thickness of the mixing layer can be obtained.

The velocity profile and the temperature profile above are given in terms of the internal coordinate system (x,y) which is related to the reference coordinate system (X,Y) by

$$Y = y - y_m$$

The jet boundary in the mixing layer is denoted by j (see Figure 5). The points for which $y=y_j$ separate the mixing layer into two regions: the mass flow rate in the range from η_j to η_{Ra} is exactly the portion of the mass flow rate of the primary flow entering the mixing layer; and the mass flow rate between η_j and η_{Rb} is exactly the portion of the mass flow rate of the secondary flow entering the mixing layer.

y_j is solved by the principle of conservation of mass and momentum before and after the mixing:

$$[illegible] \qquad (22)$$

$$[illegible] \qquad (23)$$

$$[illegible] \qquad (24)$$

where c = Crocco's number,

$$[illegible] \qquad (25)$$

y_m is also determined by the principle of conservation of mass and momentum. In terms of the similarity coordinate:

$$\eta_m = \frac{\sigma y_m}{x} = \eta_m - \frac{1}{1-\varphi_0}[I_1(\eta_m) - \varphi_0 J_1(\eta_m)] \qquad (26)$$

Analogous to the displacement thickness concept of the boundary layer, the secondary flow displacement thickness δ^*_{mix} of the mixing layer is found to be

$$-\sigma \frac{\delta^*_{mix}}{x} = \frac{\sigma \eta_2}{\eta_0} = \frac{\left(\frac{T_1^0}{T_2^0}\right) - c_1^2\varphi_1^2}{(1-c_1^2)\varphi_0} I_1(\eta_1) - \eta_m \qquad (27)$$

where $\sigma = \left[\frac{\sigma}{\sigma_1}\right]\cdot\sigma_1$,

$$\sigma_1 = 12 + \frac{2.758\cdot C_{01}}{\sqrt{(1-C_{01}^2)^{\frac{k_1-1}{k}}}}, \qquad (28)$$

$$K_1 = \frac{K_2 + \frac{2}{3}\frac{G_3\sqrt{T_3^0}}{G_2\sqrt{T_2^0}}}{1 + \frac{2}{3}\frac{G_3\sqrt{T_3^0}}{G_2\sqrt{T_2^0}}} \qquad (29)$$

$$\frac{\sigma}{\sigma_1} = \frac{1+\varphi_0}{1-\varphi_0} \qquad (30)$$

$$C_{01} = \frac{C_2^2(1-\varphi_0^2)}{C_2^2(1-\varphi_0)^2 + (1-C_2^2)}$$

Key: 1--mix; 2--secondary; 3--primary

(2) Calculation of the displacement thickness $\delta^*_{b.l.}$ of the boundary layer along the inner wall of the shroud

The effect of the boundary layer displacment thickness $\delta^*_{b.l.}$ along the inner wall of the shroud on the secondary flow rate is estimated. The properties of the boundary layer are calculated based on the equivalent length which is defined as:

$$X = (G y^\beta)^{-1}\int_0^x (G y^\beta)\,dx \qquad (31)$$

where $G = \left(\frac{M}{1+0.2M^2}\right)^4$

β is taken as 1.20 or 1.25, depending on the Reynold's number. Given the stagnation pressure and the stagnation temperature, the local Reynold's number can be calculated:

$$R_e = \frac{\sqrt{k_R R T^*}}{\nu^*} M_e (1 + 0.2 M_e^2)^{-[illegible]} \qquad (32)$$

where $$\nu^* = 9.8 \cdot 10^{[illegible]} R \frac{\mu(T^*)}{p^*} \qquad (33)$$

The displacement thickness $\delta^*_{b.l.}$ and the momentum thickness θ can then be calculated in terms of the local Reynold's number R_x. If R_x is of the order 10^6, they are found to be

$$\delta^*_{[illegible]} = 0.046 \cdot x \cdot (1 + 0.8 M_e^2)^{[illegible]} \cdot R_x^{[illegible]} \qquad (34)$$

$$\theta = 0.036 \cdot x \cdot (1 + 0.1 M_e^2)^{[illegible]} \cdot R_x^{[illegible]} \qquad (35)$$

1--b.l.

If R_x is of the order 10^7, they are.expressed by:

$$\delta^*_{[illegible]} = 0.026 \cdot x \cdot (1.0 + 0.8 M_e^2)^{[illegible]} \cdot R_x^{[illegible]} \qquad (36)$$

$$\theta = 0.022 \cdot x \cdot (1.0 + 0.1 M_e^2)^{[illegible]} \cdot R_x^{[illegible]} \qquad (37)$$

1--b.l.

The above equations are valid for K = 1.4.

Since the static pressure in the boundary layer is assumed to be a constant, the pressure on the surface δ^* is always taken as a criterion for iteration during the calculation. Hence, the calculation for the points inside the boundary layer is of the same standard form as that for the points on the surface.

4. Calculation of the thrust parameter [5]

The thrust of the engine is expressed by the following relation:

$$R = \frac{G}{g} V_e + p_e A_e - p_H A_e - \frac{G}{g} V_\infty = R_a - \frac{G}{g} V_\infty \qquad (38)$$

where R_a is the total thrust

$$R = F_a - p_H \cdot A_e \qquad (39)$$

According to the momentum theorem, the above equation can be rewritten as

$$R_a = F + F_e + R_{f} - p_H A_e \qquad (40)$$

$$F_{[illegible]} = [illegible] (1.0 + K C_{[illegible]} \cdot C_v \cdot M_{[illegible]}^2) A_{[illegible]} \cdot [illegible] \qquad (41)$$

$$F_e = p_e \cdot A_e (1.0 + K_e \cdot M_e^2) C_{[illegible]} \qquad (42)$$

in which

$$R_{[illegible]} = \int_0^{[illegible]} [illegible] \, dx \qquad (43)$$

where C_f - fictitious coefficient of the shroud

C_p - flow rate coefficient of the primary nozzle

C_v - velocity coefficient of the primary nozzle

y - radius of the shroud wall

If the viscous effect is neglected, the flow rate coefficient and the velocity coefficient of the primary nozzle are obtained by the following expressions respectively:

$$C_D = \frac{\int 2\pi y(\cos\phi dy - \sin\phi dx)}{\int 2\pi y dy} \qquad (44)$$

$$C_V = \frac{\int 2\pi y(\cos\phi dy - \sin\phi dx)\cos\phi}{\int 2\pi y(\cos\phi dy - \sin\phi dx)} \qquad (45)$$

in which the integrations are taken along the sonic line.

If the viscous effect is taken in account, the flow rate coefficient and the velocity coefficient of the primary nozzle are found by:

$$C_D = (1.0 - K_1 \cdot R_c^{-0.5}) \frac{\int 2\pi y(\cos\phi dy - \sin\phi dx)}{\int 2\pi y dy} \qquad (46)$$

$$C_V = (1.0 - K_2 \cdot R_c^{-0.5}) \frac{\int 2\pi y(\cos\phi dy - \sin\phi dx)\cos\phi}{\int 2\pi y(\cos\phi dy - \sin\phi dx)} \qquad (47)$$

where

$$K_1 = \frac{0.15\sqrt{2}}{\sin\phi_c}, \quad K_2 = 0.141.$$

and ϕ_c - semi-vertex angle of the primary nozzle
ϕ - angle between the flow velocity on the sonic line and the x-axis
y - radial coordinate of the points on the sonic line
x - axial coordinate of the points on the sonic line
R_c - Reynold's number

COMPARISON BETWEEN THE NUMERICAL AND THE EXPERIMENTAL RESULTS

A program for the numerical method proposed here has been developed and the flow field, pressure distribution along the nozzle wall and the pumping characteristic of the ejector nozzle are calculated. The comparison between computed results and experimental data are summarized below:

1. The flow field and the pressure distribution along the wall of the ejector nozzle

The input data are:

NW = 18 total number of node points on the shroud
N2 = 20 number of points taken along the sonic line
N1 = 29 number of expansion waves taken as the characteristics net

N4 = 100 upper limit of the iterative variable J

XW = 0 x coordinate of the shroud at the exit plane of the primary nozzle

XC = 0 x coordinate of free jet at the exit plane of the primary nozzle

YC = 0.045 m radius of the primary nozzle at the exit plane

V = 0.88 kg/s mass flow rate of the secondary flow

G_a=14.4258 kg/s mass flow rate of the primary flow

p_b^* = 30702 kg/m stagnation pressure of the secondary flow

T_b^* = 288 K stagnation temperature of the secondary flow

K_b = 1.4 specific heats ratio of the secondary flow

R_b = 29.27 kg-m/kg K gas constant of the secondary flow

T_a^* = 288 K stagnation temperature of the primary flow

p_a^* = 97992 kg/m stagnation pressure of the primary flow

R_a = 29.27 kg-m/kg K gas constant of the primary flow

X_H = 0.090 m distance from the exit of the primary nozzle to the exit of the shroud

K_a = 1.4 specific heat ratio of the primary flow

p_H = 10333 kg/m ambient pressure

Input data for the shroud profile are:

XS = X/YC	*WS = Y/YC*	*XS = X/YC*	*WS = Y/YC*
0	1.2780	0.6889	1.1289
0.1111	1.2458	0.7556	1.1394
0.2222	. 2133	0.8222	1.1424
0.3333	1.1809	0.8889	1.1542
0.3778	1.1680	1.1111	1.1933
0.4444	1.1511	1.3333	1.2324
0.4889	1.1411	1.5556	1.2710
0.5556	1.1341	1.7780	1.3107
0.6222	1.1267	2.0000	1.3500

The output data are the pressure p, the coordinates x,y, the flow angle ϕ, mass rate of flow of the secondary flow GS and other necessary parameters at all points of the characteristics net.

The characteristics of the ejector nozzle obtained are shown in Figure 6.

Figure 6. Characteristics of the ejector nozzle

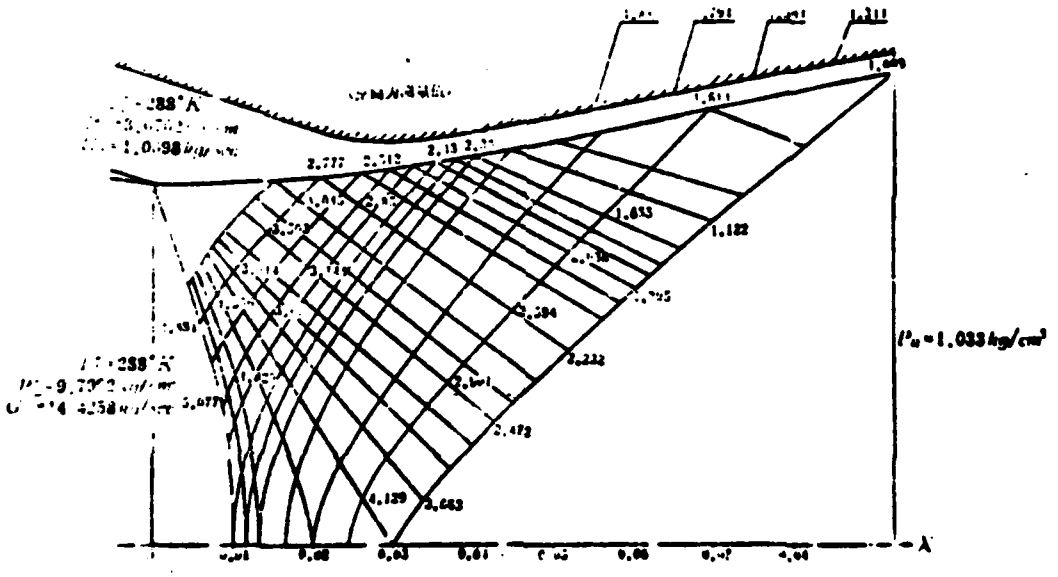

The computed values and the experimental data of the pressure distribution along the shroud are shown in Figure 7.

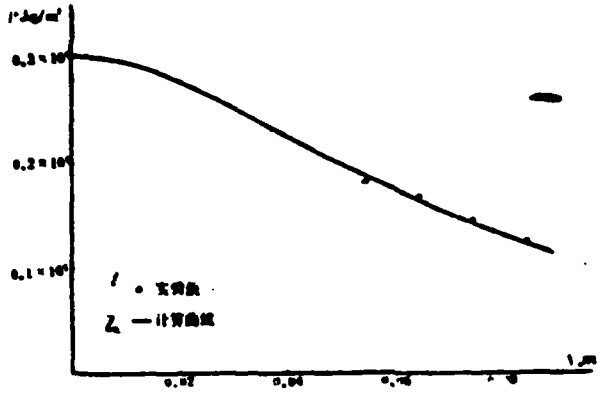

Figure 7. Pressure distribution along the shroud
Key: 1--experimental data; 2--calculated curve

2. Pumping characteristic of the ejector nozzle

In Figure 8, curve 1 is the computed result for inviscid flow, and curve 2 is the corrected result for viscous flow. The figure indicates that the computed result after correction for the viscous effect is in good agreement with the experimental data.

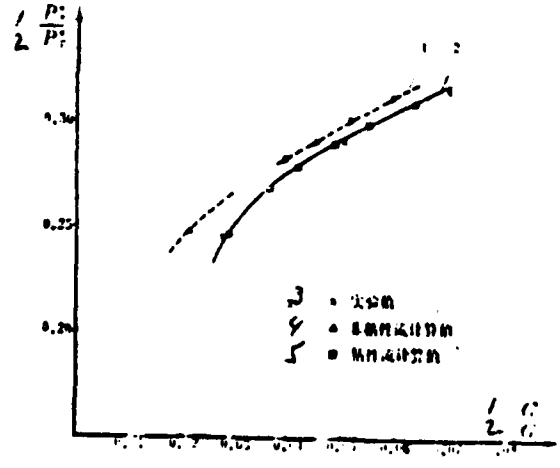

Figure 8. Pumping characteristic of the ejector nozzle
Key: 1--secondary; 2--primary; 3--experimental data; 4--calculated values of inviscid flow; 5--calculated values of viscous flow

Figure 8 also indicates that for the condition of high secondary flow rate, the error between the inviscid result and the experimental data is no more than 10%.

CONCLUSION

1. The numerical method proposed is found to be satisfactory.

2. The correction for viscous effect proposed is relatively simple but still accurate.

SYMBOLS

ψ - stream function

ρ - density

a - speed of sound

u - velocity component in the axial direction

v - velocity component in the radial direction or flow velocity at the exit of the nozzle

p - pressure

μ - Mach angle

ϕ - flow angle (angle between the streamline and the horizontal axis)

θ - angle between the characteristic and the radial axis, or the momentum thickness of the boundary layer

X - equivalent length

y - radial distance normalized by the radius of the primary nozzle

x - axial distance normalized by the radius of the primary nozzle

ω - transformed velocity

α - semi-conical angle of the primary nozzle at the exit

T - temperature

G - mass flow rate

M - Mach number

λ - velocity coefficient of the flow

K - specific heat ratio

R - thrust or gas constant or radius

A - area

F - impuse or functional relation

η - coordinate along the Mach line

ξ - coordinate along the Mach line

β - constant determined by the Reynold's number

γ^* - coefficient of viscosity expressed in terms of stagnation parameters

$\delta^*_{b.l.}$ -displacement thickness of the boundary

Subscripts:

primary, a - primary flow

secondary, b - secondary flow

C - exit of the primary nozzle

e - exit plane of the ejector nozzle

H - ambient condition

G - total

C - total

O - inlet of the ejector nozzle

SH - shroud

Superscript: * - stagnation

REFERENCES

[1] Hardy, J. M., E'tude Th.orique d'une Tuvère Convergente-Divergente Bi-Flux. L'Aéronautique et l'Astronautique. No. 37. 1972-5. pp. 25-37.

[2] Hardy, J. M., et Lacombe, H., Les Tuyères Supersoniques à Double Flux. Méthodes de Calcul. Revue Française de Mécanique. No. 24. 4 trimestre. 1967. pp. 49-59.

[3] Anderson, B. H., Computer Program for Calculating the Field of Supersonic Ejector nozzles. NASA TND-7601. 1974. pp 1-86.

[4] Chow, W. L., and Addy, A. L., Interaction between Primary and Secondary Streams of Supersonic Ejector Systems and Their Performance Characteristics. AIAA Journal. Vol. 2. No. 4. April 1964. pp 686-695.

[5] Korst, H. H., Addy, A. V., and Chow, W. L., Installed Performance of Air-Augmented Nozzles Based on Analytical Determination of Internal Ejector Characteristics. Journal of Aircraft. Vol. 3. No. 6. Nov.-Dec. 1966. pp. 498-506.

[6] Carriere, P., Exhaust Nozzles. Supersonic Turbo-jet propulsion Systems and Components. AGARD graph No. 120. 1969. pp. 287-374.

[7] Anderson, B. H., Factors which Influence the Analysis and Design of Ejector Nozzles. AIAA. Paper 72 46. Jan. 1972.